© 2019. Published by The Company of Biologists Ltd | Journal of Experimental Biology (2019) 222, jeb198226. doi:10.1242/jeb.198226

RESEARCH ARTICLE

Quantifying the swimming gaits of veined squid (*Loligo forbesii*) using bio-logging tags

Genevieve E. Flaspohler[1,2], Francesco Caruso[3,4], T. Aran Mooney[3,*], Kakani Katija[5], Jorge Fontes[6,7,8], Pedro Afonso[6,7,8] and K. Alex Shorter[9]

ABSTRACT

Squid are mobile, diverse, ecologically important marine organisms whose behavior and habitat use can have substantial impacts on ecosystems and fisheries. However, as a consequence in part of the inherent challenges of monitoring squid in their natural marine environment, fine-scale behavioral observations of these free-swimming, soft-bodied animals are rare. Bio-logging tags provide an emerging way to remotely study squid behavior in their natural environments. Here, we applied a novel, high-resolution bio-logging tag (ITAG) to seven veined squid, *Loligo forbesii*, in a controlled experimental environment to quantify their short-term (24 h) behavioral patterns. Tag accelerometer, magnetometer and pressure data were used to develop automated gait classification algorithms based on overall dynamic body acceleration, and a subset of the events were assessed and confirmed using concurrently collected video data. Finning, flapping and jetting gaits were observed, with the low-acceleration finning gaits detected most often. The animals routinely used a finning gait to ascend (climb) and then glide during descent with fins extended in the tank's water column, a possible strategy to improve swimming efficiency for these negatively buoyant animals. Arms- and mantle-first directional swimming were observed in approximately equal proportions, and the squid were slightly but significantly more active at night. These tag-based observations are novel for squid and indicate a more efficient mode of movement than suggested by some previous observations. The combination of sensing, classification and estimation developed and applied here will enable the quantification of squid activity patterns in the wild to provide new biological information, such as *in situ* identification of behavioral states, temporal patterns, habitat requirements, energy expenditure and interactions of squid through space–time in the wild.

KEY WORDS: Persistent monitoring, Gait, Movement patterns, Energetics, Biotelemetry

[1]Applied Ocean Physics and Engineering Department, Woods Hole Oceanographic Institution, Woods Hole, MA 02543, USA. [2]Computer Science & Artificial Intelligence Laboratory, Massachusetts Institute of Technology, Cambridge, MA 02139, USA. [3]Biology Department, Woods Hole Oceanographic Institution, Woods Hole, MA 02543, USA. [4]Marine Mammal and Marine Bioacoustics Laboratory, Institute of Deep-Sea Science and Engineering, Chinese Academy of Sciences, Sanya, 572000, China. [5]Research and Development, Monterey Bay Aquarium Research Institute, 7700 Sandholdt Road, Moss Landing, CA 95039, USA. [6]MARE – Marine and Environmental Sciences Centre, R. Frederico Machado, 9901-862 Horta, Faial, Azores, Portugal. [7]IMAR- Institute of Marine Research, University of the Azores, 9901-862 Horta, Faial, Azores, Portugal. [8]Okeanos – University of the Azores, 9901-862 Horta, Faial, Azores, Portugal. [9]Department of Mechanical Engineering, University of Michigan, Ann Arbor, MI 48109, USA.

*Author for correspondence (amooney@whoi.edu)

F.C., 0000-0001-6881-3786; T.A.M., 0000-0002-5098-3354

Received 12 December 2018; Accepted 16 October 2019

INTRODUCTION

Squid are diverse and ecologically important marine organisms. As squid are ectothermic animals, their physiology and behavior can be directly linked to the physical conditions of their surrounding environment (Kaplan et al., 2013; Rosa and Seibel, 2010). In turn, squid behavior and habitat use can have substantial impacts on marine ecosystems and fisheries. Monitoring and observing squid behavioral patterns and vital rates can be important for understanding their activity and energy usage (O'Dor et al., 1995; Pörtner, 2002), as well as for elucidating the broader ecological interactions between squid and the taxa they influence (e.g. foraging rates; Clarke, 1977) and how environmental changes may alter these activities (Pörtner et al., 2004; Rosa et al., 2014).

Because of the inherent difficulties of working in the marine environments inhabited by squid, experiments and observation conducted in controlled environments have been used to generate important information about how these animals move in their natural environment. Early captive experiments demonstrated that squid are highly maneuverable and create propulsive forces for locomotion using a combination of fin motion and jet propulsion (O'Dor and Webber, 1986). Many cephalopods have been shown to use their fins for locomotion that requires fine-scale maneuverability, and rely on jet propulsion for sudden bursts of speed required to evade a predator (Bartol et al., 2001). By combining finning and jetting, these animals can also generate different swimming gaits (Anderson and DeMont, 2000; Anderson and Grosenbaugh, 2005; Bartol et al., 2016, 1999; O'Dor, 1988; Stewart et al., 2010).

Observed gaits range from a smooth translational gait generated by moving the fins in an undulatory–sinusoidal pattern to a flap-and-glide gait used to increase speed and acceleration during jet-propelled fast swimming maneuvers (Bartol et al., 2009). These gaits may also occur in tandem (i.e. low level jetting in combination with finning or flapping). Additionally, the habitat and species behavior seem to influence the predominant gaits that an animal utilizes. For example, squid like *Illex illecebrosus* that swim at moderate to high speeds in the wild may rely heavily on jetting for propulsion (O'Dor et al., 1995). In contrast, the shallow-water brief squid, *Lolliguncula brevis*, demonstrates a complex locomotive repertoire and a high degree of maneuverability enabled by fin propulsion (Bartol et al., 2001; Jastrebsky et al., 2017, 2016). However, there are approximately 700 species of squid and only a small number of species have been involved in these studies. Deep-water animals and those that live in more extreme environments are hard to collect and maintain in captivity, and likely differ in behavior and physiology from their shallow-water counterparts. Thus, for many species of squid, movement data may be best obtained via observations in their natural environment.

Squid are generally considered to operate near their metabolic limit (Pörtner, 2002) and their jet propulsion and escape jets are considered a high-cost locomotion mode (O'Dor and Webber, 1991;

Journal of Experimental Biology (2019) 222, jeb198226. doi:10.1242/jeb.198226

List of symbols and abbreviations

$\mathbf{A}^{(t)}=[A_x^{(t)}\ A_y^{(t)}\ A_z^{(t)}]^T$	components of acceleration in the tag frame at time step t
$\mathbf{A}_s^{(t)}=[A_{x,s}^{(t)}\ A_{y,s}^{(t)}\ A_{z,s}^{(t)}]^T$	components of static acceleration in the tag frame at time step t
$\mathbf{A}_d^{(t)}$	vector of dynamic (movement-induced) acceleration at time t
$\mathbf{A}_s^{(t)}$	vector of static (orientation-induced) acceleration at time t
IQR	interquartile range
ODBA	overall dynamic body acceleration
ε_l, ε_h	animal-specific low and high threshold, respectively, for pitch classification
$\theta^{(t)}$	pitch of the animal at time step t

O'Dor et al., 1995). Together with the necessary lift (for dense, muscular squid) and drag, many squid have, to some extent and at least historically, been considered inefficient swimmers (O'Dor, 1988). Yet, efficient swimming patterns are likely vital to their survival and subsequent ecological interactions. Consequently, it has been suggested that they must use behavioral trade-offs (such as gliding on currents) to be successful swimmers (O'Dor et al., 2002; O'Dor and Webber, 1991). Laboratory observations of *Loligo opalescens* and depth data from tagged pelagic Humboldt squid, *Dosidicus gigas*, suggest these animals use a climb-and-glide behavior when swimming. For *D. gigas*, this behavior has been observed when vertically migrating or transiting in and above oxygen minimum zones, with jetting suggested to be a regularly occurring behavior which enables the climb (Gilly et al., 2006; O'Dor, 1988). In contrast, pressure sensors integrated into tags applied to *Loligo forbesii* indicated that maximal aerobic jetting was infrequent and jetting was often observed in combination with finning (O'Dor et al., 1995), suggesting that this benthic-oriented deep-water squid might rely on diverse combinations of jetting- and finning-based swimming modes during daily movements and migrations. Laboratory studies of movement in *L. brevis* show a predominant use of finning modes to generate lift and thrust for propulsion at a variety of speeds (e.g. Bartol et al., 2008; Stewart et al., 2010). In these studies, researchers also observed fluid flow from the siphon during finning, which is innately linked to respiration and mantle contraction. Yet, such studies are typically confined to small flumes, limiting squid movements in order to accurately observe locomotion. Thus, there is still some uncertainty regarding how squid may move in an open environment, and the relative proportions of gait behaviors. Such an understanding of squid movement could provide insight into why this taxon is so successful. Identifying these behaviors *in situ* requires fine-grained concurrent environmental and behavioral measurements in order to better understand squid behavioral physiology and the impacts of environmental forces on squid survival.

Early attempts to study squid in their natural environment using biologging tags employed acoustic pingers to actively track squid and quantify vertical and horizontal movements in the water column (O'Dor et al., 1995). From these and other studies, activity patterns indicated that tidal currents were a key environmental influence, and were as important as temperature, diel cycles and foraging behavior (O'Dor et al., 2002; Stark et al., 2005). Large *D. gigas* were successfully tagged using temperature–depth satellite transmitting tags (~1 Hz resolution) and 'Crittercam' video packages (Gilly et al., 2006, 2012; Stewart et al., 2013). During these deployments, vertical casts using a conductivity, temperature and depth (CTD) logger with oxygen sensor were made in the general location of the tagged animals. From these data, it was apparent that the swimming depths of *D. gigas* were greatly influenced by the temperature or dissolved oxygen in the water column, although it is difficult to conclusively link measured animal behavior to environmental conditions because of the decoupled environmental and animal behavioral measurements. These data provided a unique insight into the behaviors of a large, ecologically important squid, but the types of sensors and the sampling rates of these tags were not able to capture fine-scale behaviors like respiration, swimming (finning and jetting) or foraging events (Broell et al., 2013). The identification and classification of squid swimming gaits, along with associated environmental data, have the potential to aid in our understanding of squid swimming patterns and behavior in the wild, which has implications for understanding their activity budgets, estimated energetic cost and trade-offs for survival.

Bio-logging technology has dramatically improved over the past several years. Tags are increasingly able to measure a range of movement, acoustic, physiological and environmental parameters at high sampling rates for days or weeks at a time (Block, 2005; Bograd et al., 2010; Costa et al., 2010; Hussey et al., 2015). However, given access to these high-resolution datasets, it becomes necessary to develop classification and estimation algorithms that can efficiently extract behavioral information and allow for effective analysis (Nathan et al., 2012; Shorter et al., 2017). This combination of sensing, classification and estimation enables the quantification of organismal activity patterns that provide critical biological information, such as identification of behavioral states, temporal patterns, habitat requirements, estimated energy expenditure and community interactions (e.g. reproductive activity or predator-prey events). Thus, the development and evaluation of classification and estimation technologies in a controlled environment are an essential first step in establishing the accuracy and viability of the algorithms before they are used on data from an environment where behavioral state cannot be monitored directly.

In this work, we present novel data and analysis algorithms that can be used to identify and classify squid swimming behavior from an animal-borne bio-logging tag, the ITAG (Mooney et al., 2015). Data collection and algorithm development were conducted with animals in a controlled environment, enabling a detailed evaluation of the developed tools and insight into the relative proportions of locomotive modes (i.e. finning, flapping, jetting). Measurements of movement, orientation and environmental conditions (temperature, ambient light, pressure) at high temporal resolution were collected to measure characteristics of squid locomotion *in vivo* and develop a robust estimator for an animal's activity level and gait based on overall dynamic body acceleration (ODBA) (Wilson et al., 2006). Synchronized video recordings of the tagged squid were then used to build gait and orientation classifiers that were applied to the data collected in tank experiments to draw conclusions about representative swimming strategies of captive animals. The data reveal that this large, negatively buoyant squid predominantly uses finning-based swimming modes which enabled lower overall ODBA (compared with jetting alone), suggesting a tendency toward efficient swimming modalities. The algorithmic and data-processing techniques developed in this work can serve as the foundation for data-driven predictors of the patterns used by animals *in situ*.

MATERIALS AND METHODS

Experimental facilities and equipment

Trials were conducted with captive squid between 15 March and 1 April 2014 at the Porto Pim Aquarium, a public facility run by Flying Sharks on Faial Island, Azores, Portugal. Healthy, adult *L. forbesii* Steenstrup 1856 squid with a mean (±s.d.) mantle length of

Journal of Experimental Biology (2019) 222, jeb198226. doi:10.1242/jeb.198226

58±4.0 cm (range 52–69 cm) were collected at the nearby island slope (approximately 200 m depth) by hand jigging. Upon capture, animals were immediately brought back to the aquarium facility and maintained in a large 8 m×4 m×4 m (L×W×D) observation tank containing filtered seawater pumped from the adjacent Atlantic Ocean. Approximately 30–60 min prior to tagging, animals were transferred to flexible, soft containers with a diameter and depth of 1.5 m (Mooney et al., 2015). ITAGs were attached dorsally on eight individual squid near the posterior of the mantle with sutures (Fig. 1).

The ITAGs are neutrally buoyant bio-logging tags bearing a three-dimensional (3D) accelerometer, 3D magnetometer, and pressure and light sensors within an epoxy and syntactic foam housing. The tag dimensions were 108.4 mm×64.0 mm×28.7 mm (L×W×H). Data from all sensors were recorded at a sample rate of 250 Hz to internal flash memory. The accelerometer and magnetometer sense movement and are used to calculate animal locomotion and orientation (pitch, roll and yaw); the pressure sensor measures the depth of the animal; and the light sensor measures ambient light levels in the tank during the experiment (see Mooney et al., 2015, for a detailed description). After tag attachment and subsequent acclimation period, animals were released into a large 8 m×4 m×4 m (L×W×D) observation tank containing filtered seawater. Immediately after release, the tagged and untagged squid exhibited similar coloration patters, body positions, and interactions with conspecifics and other fishes, including tope sharks (*Galeorhinus galeus*) and smaller 'prey' fish (Fig. 1). The tags separated from the animals using a timed-release mechanism. The mean duration of ITAG recordings was 20:43:51 (h:min:s) but some recordings exceeded 24 h.

In addition to tag data, three overhead, high-definition video cameras (GoPro Hero3, San Mateo, CA, USA; 1920×1080 resolution, 30 frames s^{-1}) and two side-looking high-definition video cameras (Sony HDR-XR550, Tokyo, Japan; 1920×1080 resolution, 60 frames s^{-1}) located at the ends of the tank were used to record portions of the tag trials. The video cameras were synchronized using successive flashes of light (via an external camera flash; Canon, Melville, NY, USA), and tag data were synchronized to the video by recording the arming of the tag (and its flashing LEDs) with one of the five video cameras. The video data were scored by an observer to identify squid behaviors using the side-looking cameras, which provided information on fin amplitude, shape, and frequency of the wave along the fin chord. These human behavioral annotations were used to develop the classification algorithms, which in turn were used to analyze the ITAG sensor data. The scored behaviors included finning, flapping and jetting, as well as arms- versus mantle-first direction of travel.

After tags were recovered, the data were offloaded and decompressed for analysis using the DTAG toolbox for MATLAB (Johnson and Tyack, 2003), with all subsequent data analysis performed in MATLAB 2016b (MathWorks, Cambridge, MA, USA). The pressure sensor on one out of the eight deployments malfunctioned and did not produce viable pressure measurements, and this tag was excluded from further analysis. From analysis of the original 250 Hz data, finning frequencies of *L. forbesii* were determined to be approximately 1 Hz using Fourier analysis of the raw accelerometry data from the portions of the data classified as finning. Rapid motions, such as maximal escape jet propulsion, occurred at a frequency no higher than 10 Hz (0.1 s event duration) across all animals. The original data (sampled at 250 Hz) were decimated to 25 Hz for further analysis. This sampling rate was above the sample rate necessary to capture squid movements and is commensurate with the 'high-frequency' rate recommended by Broell et al. (2013) in order to minimize aliasing when classifying animal behavior using accelerometry data.

Estimating specific acceleration

Overall dynamic body acceleration (ODBA) was used to separate the animals' overall accelerometry signal into estimates of specific acceleration generated by locomotion and gravitational acceleration caused by animal orientation (Gleiss et al., 2011). This method uses a moving average filter to separate high-frequency dynamic accelerations, corresponding to animal gait and movement, from lower frequency changes in accelerometry, corresponding to changes in animal orientation. The size of the window used in the moving average filter was set to 50 samples for the ITAG (Fig. 2B; following Shepard et al., 2008). The ITAG acceleration data at timestep t were then split into three component accelerations: $\mathbf{A}^{(t)}=[A_x^{(t)}\,A_y^{(t)}\,A_z^{(t)}]^T$; and

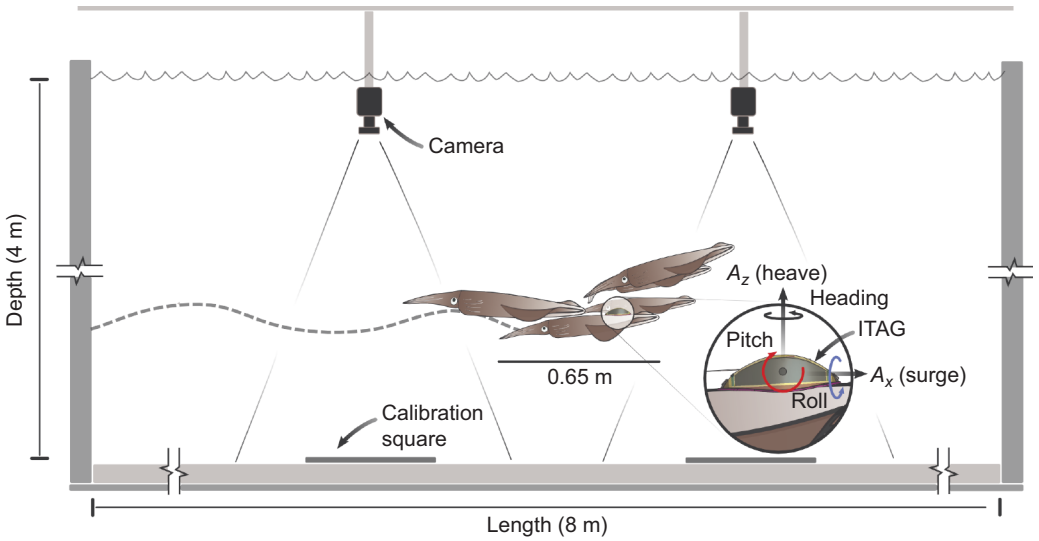

Fig. 1. Experimental setup. 8 m×4 m×4 m (L×W×D) holding tank was used for squid high-resolution bio-logging tag (ITAG) experiments at the Porto Pim Aquarium (Azores, Portugal). Three overhead high-definition video cameras and two side-looking high-definition video cameras (located at the ends of the holding tank) concurrently recorded behaviors of tagged veined squid. Calibration squares were located at the bottom of the tank to facilitate the recognition of different squid behaviors, assist with the identification of squid differing in size and analyze the speed of movements during the video analysis.

Journal of Experimental Biology (2019) 222, jeb198226. doi:10.1242/jeb.198226

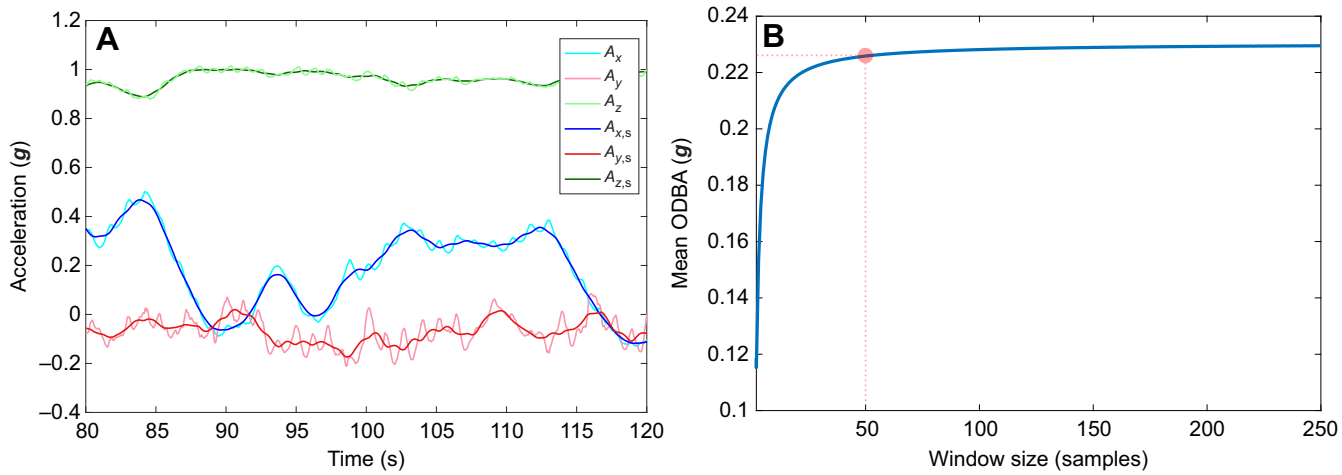

Fig. 2. Methods. (A) Separating the dynamic acceleration signal from the static acceleration signal. The original acceleration components $\mathbf{A}^{(t)}=[A_x^{(t)}A_y^{(t)}A_z^{(t)}]^T$ from t=80.0 s to t=120.0 s are shown in light blue, red and green, respectively. After applying a moving average filter to each vector, the resulting signal represents the static (orientation-induced) acceleration signal $\mathbf{A}_s^{(t)}=[A_{x,s}^{(t)}A_{y,s}^{(t)}A_{z,s}^{(t)}]^T$ in dark blue, dark red and dark green, respectively. The dynamic (or movement-induced) acceleration signal was calculated as the component-wise absolute difference between the original signal and the static signal: $[\mathbf{A}_d^{(t)}=|\mathbf{A}^{(t)}-\mathbf{A}_s^{(t)}|]$. (B) The size of the moving average filter was selected such that the average overall dynamic body acceleration (ODBA) value across the dataset ceased to be sensitive to changes in window size, following the method in Shepard et al. (2008). We found this point to be approximately 50 samples, or 2 s of data at 25 Hz.

a moving average filter was applied to each component. The resulting signal represented the static (orientation-induced) acceleration signal $\mathbf{A}_s^{(t)}=[A_{x,s}^{(t)}A_{y,s}^{(t)}A_{z,s}^{(t)}]^T$. The dynamic (movement-induced) acceleration at timestep t was calculated as the component-wise difference between the original signal and the static signal: $\mathbf{A}_d^{(t)}=|\mathbf{A}^{(t)}-\mathbf{A}_s^{(t)}|$ (Fig. 2A).

Gait analysis

The focus of this study was to discern the relative locomotive modes (gaits) used by *L. forbesii* and subsequently define a gait classification pipeline based on dynamic acceleration that can be readily extended to wild squid studies. Previous literature has shown that squid use a combination of fin movement and jet propulsion both concurrently and separately to move through the water (Bartol et al., 2001). Stewart et al. (2010) also demonstrated that *L. brevis* use their fins in different modes to generate propulsive forces, along with their jet, during locomotion. In our experiments, trained observers identified visually distinct swimming gaits from video data of tagged, tank-bound squid, and features extracted from the tag sensor data were used to develop a classification algorithm for these visually distinct gaits.

The gait classifier used the absolute magnitude of the estimated dynamic acceleration and the average power spectral density of the dynamic acceleration as features to identify the three classes of squid gaits observed during our trials: (1) finning, (2) flapping and (3) jetting. The finning and flapping gaits loosely correspond to the mode II and mode III/mode IV squid gaits introduced by Stewart et al. (2010). The low-acceleration finning gait was characterized by slow, undulatory motion of the fins with at least one full wavelength of undulation present along the fin chord and little observable contribution from jetting propulsion. The intermediate-acceleration flapping gait was characterized by a full flapping motion of the fins, in which the fins on each side of the mantle move upwards and downwards simultaneously and with approximately equivalent upstroke and downstroke periods. Flapping was associated with higher swimming speeds than the finning gait. Finally, the high-acceleration jetting gait was characterized by rapid acceleration with the fins tucked alongside the squid mantle (no fin contribution) and observable jet propulsion. Although *L. forbesii* are known to employ jet propulsion in combination with fin propulsion during locomotion (O'Dor et al., 1995), our use of non-invasive, biologging tags for gait detection did not readily allow for the contribution of fin- versus jet-based propulsion to be disentangled in the three observed gaits.

The gait classifier uses the dynamic acceleration signal as an input and labels all samples within a sliding window of length N as one of the three possible gaits. We selected this window size of 25 points to match the fundamental frequency of dynamic accelerations of the slowest observed gait present in the dataset, i.e. finning, which was an approximately 1 Hz signal. Our analysis used the peak ODBA magnitude and the average power spectral density in each window to classify gait using a decision tree classifier (Kotsiantis, 2013) (see Fig. 3 and Fig. 4A). These features were chosen because preliminary analysis of the data showed that the dynamic acceleration signal exhibited different magnitudes and frequencies for the three gaits. Finning was correlated with low ODBA magnitude and a low spectral density concentrated near 1 Hz; flapping was correlated with higher ODBA and spectral density in moderate frequency range (2–5 Hz); jetting had high ODBA peaks and high overall spectral density with frequency components in the 5–10 Hz range.

To build an automated gait classifier, gait events were manually labeled in the 64 overhead video clips of tagged animals, for a total 1232 s of labeled behavior across the seven tagged individuals. Data from both the overhead and lateral cameras were used to score the observed gait. Half of the video clips (635 s) were used to fit the parameters of the gait classifier (the training dataset); the other half (597 s) were held out and used to validate the generalizability of the classifier to unseen data (the testing dataset).

To perform gait classification, we used a decision tree classifier (Kotsiantis, 2013) to place each 1 s-long gait window into a finning, flapping or jetting gait category. Decision tree classifiers are often applied in small data domains and in scientific applications because of their low model complexity and interpretability. The decision tree was fitted on the training dataset using MATLAB's fitctree method (MATLAB 2016b) with default parameters and pruning level. For each 1 s-long window, the peak ODBA acceleration was extracted using MATLAB's findpeaks method and the power spectral density was computed using MATLAB's spectrogram method (window length 25 samples, Hamming window, sampling rate 25 Hz). This length–two feature vector was input into the decision tree for gait

Journal of Experimental Biology (2019) 222, jeb198226. doi:10.1242/jeb.198226

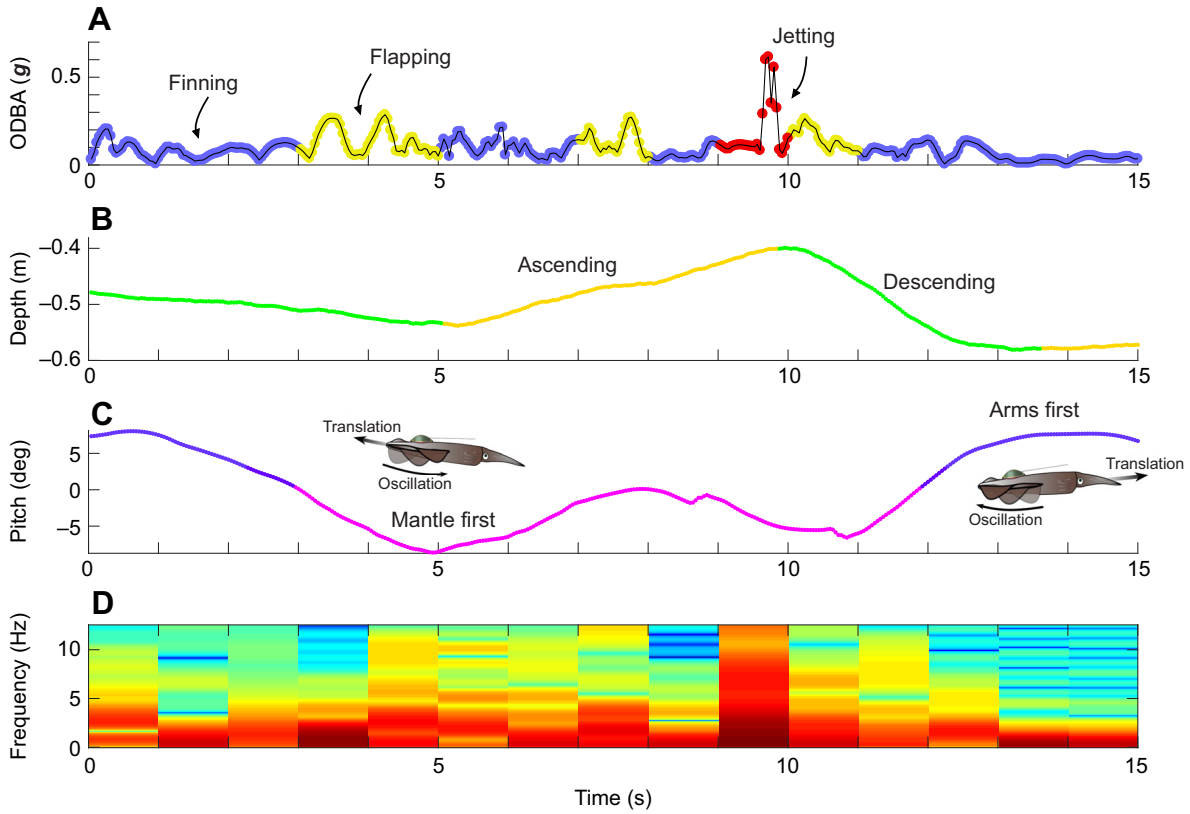

Fig. 3. Sample ITAG output. (A) An example of squid gait identification using ODBA, depth and pitch measurement; analysis of the accompanying video footage validated the automated classification results. A representative period (15 s) of swimming data illustrates the three types of identified gait: finning, flapping and jetting. These different gaits were observed in the accelerometer data and were characterized using ODBA. (B) ITAG-collected pressure data can be used to identify the vertical movement of squid in the water column (times of ascent versus descent). (C) ITAG-collected pitch data yielded animal pitch, which was used to determine the animal's orientation during swimming (e.g. arms first or mantle first). (D) The frequency response of the ODBA signal. A fast Fourier transform was run on each 1 s window of the ODBA signal. Each gait exhibits a unique frequency response, which is used in the gait classifier. For example, the jetting gait has a much higher power spectral density than the other gaits.

classification and the model parameters were optimized to maximize classifier accuracy on the training dataset. The resulting decision tree is shown in Fig. 4A, while the ODBA acceleration and spectral features are shown in Fig. 3 for a 15 s segment from the training dataset.

We then tested the accuracy and robustness of the classifier by evaluating classifier performance on an additional test dataset of paired video/accelerometry data. We ran the trained decision tree gait classifier on the clips in the testing set and recorded the label given to each gait event. The overall accuracy of the classifier was determined as the number of events in the labeled testing data that were correctly identified by the classifier, divided by the total number of labeled events in the testing video clips.

Ascending and descending motion

Pressure data provided an accurate measurement of squid depth in the tank and, similar to natural environments, squid often actively ascended and descended within the water column (Gilly et al., 2006, 2012). A moving average filter with a window size of 50 samples was used to filter the pressure data. The sign of the discrete-time derivative of the pressure data was used to discriminate between periods of ascent and descent (Fig. 3B). A squid specimen was defined as ascending if the value of the pressure measurement decreased between two subsequent measurements as descending if the pressure measurement increased. It is also possible to include a third vertical motion category for when an animal was perfectly stationary in the water column. However, this case occurred very rarely because the pressure sensor used on the ITAG device is sufficiently sensitive to capture micro-movements of the squid up and down in the water column. We therefore chose to always classify the squid as ascending or descending in the water column.

Forwards and backwards motion

Squid can travel both 'forward' (arms first) and 'backward' (mantle first). Although direction changes can be difficult to detect using accelerometer data alone, our video data revealed that squid tend to swim with the leading edge of their body at a positive angle of attack with respect to the direction of travel, such that the part of the animal (arms versus mantle) facing the oncoming flow is held vertically higher (Fig. 3C). Because the tag is mounted rigidly to the squid body, this corresponds to a positive tag pitch angle when the animal is traveling arms first and a negative tag pitch when the animal is traveling mantle first. Tag pitch was calculated using the static acceleration signal as:

$$\theta^{(t)} = \arctan\left(\frac{A_{y,\mathrm{s}}^{(t)}}{\sqrt{(A_{x,\mathrm{s}}^{2(t)} + A_{y,\mathrm{s}}^{2(t)})}}\right). \quad (1)$$

Using data and video observations, we defined swimming behavior with tag pitch greater than some high threshold ($\theta^{(t)}>\varepsilon_{\mathrm{h}}$) as forward, arms-first motion, and pitch less than some low threshold ($\theta^{(t)}<\varepsilon_{\mathrm{l}}$) as backward, mantle-first motion. Pitch angles in

Journal of Experimental Biology (2019) 222, jeb198226. doi:10.1242/jeb.198226

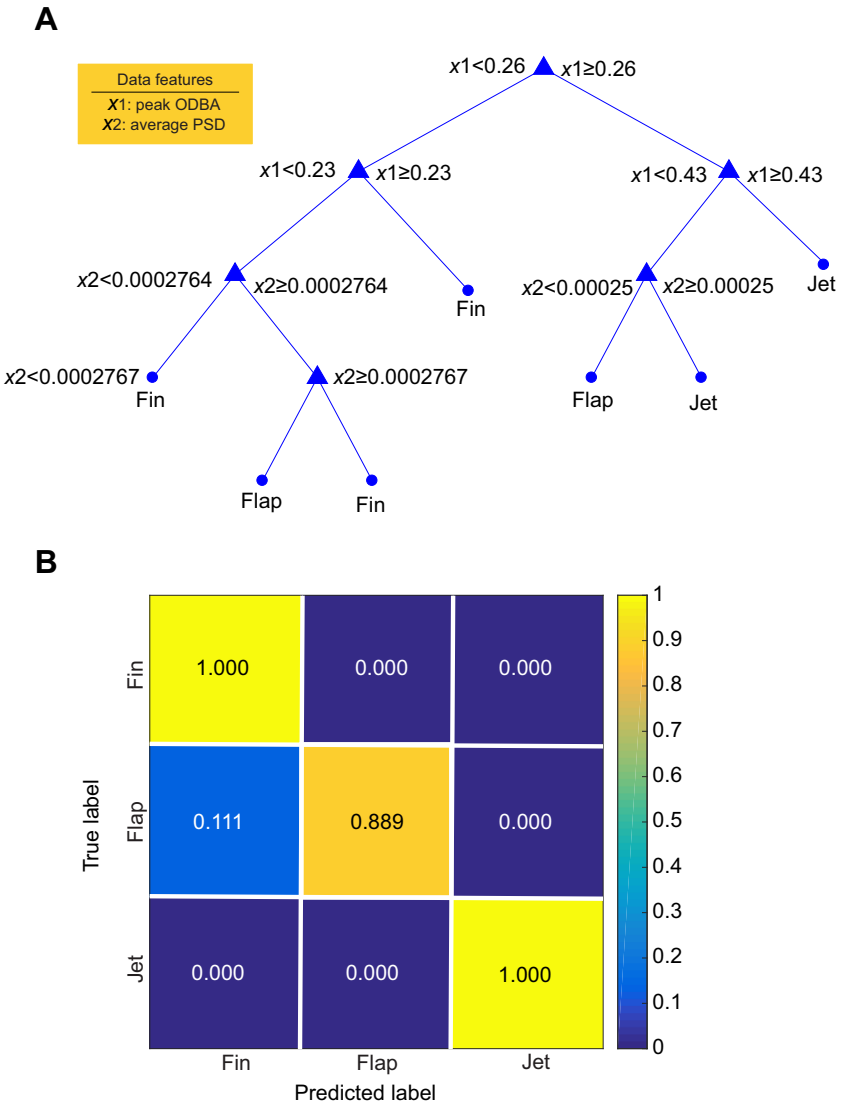

Fig. 4. Classification tree and confusion matrix. (A) The learned decision tree classifier. A two-dimensional vector containing the maximum ODBA peak and average power spectral density (PSD) in a 1 s window is input into the tree. The tree makes a series of branching linear separations, visualized as a set of branching points, and produces the gait output seen at the leaves of the tree. (B) The accuracy of the automatic detection algorithms as visualized using a confusion matrix. The three main gaits identified were finning, flapping and jetting. Sixty-four video clips (maximum and minimum durations of 73 s and 4 s, respectively; mean duration of 13 s) of tagged squid gait events were analyzed by a human operator and these results were compared with the automatic classification algorithm. The rows represent the human-labeled gaits, and the columns represent labels generated by the automatic classifier. The number in each cell corresponds to the proportion of gait events classified with a specific combination of true and predicted label. For reference, a perfect classifier would show only detections along the diagonal squares because true and predicted labels would always correspond.

the range $\varepsilon_l<\theta^{(t)}<\varepsilon_h$ were observed during squid direction changes. Because the magnitude of pitch can vary with animal swimming style or tag attachment, ε_l and ε_h were calculated as a proportion of the mean pitch ($\bar{\theta}$) observed throughout the trial ($\varepsilon_l=0.95\bar{\theta}$, $\varepsilon_h=\bar{\theta}$). These pitch thresholds were determined manually using a set of training observations from the video recordings. The accuracy of the direction of travel classification was quantified by comparing the automatic, ODBA-based direction classification with human annotations on a testing dataset containing 817 s of human-labeled squid direction behaviors.

Diel behavioral patterns

Five of the tag recordings encompassed an entire ca. 24 h period, during which animals received a natural day–night light cycle through the overhead windows. We calculated how squid behavior (e.g. gait, swimming direction, ascending/descending) and ODBA varied as light varied during the deployment. During the experiment, the squid were released into the tank after tagging a few hours before sunset and spent the night in the tank, and the tags were released from the animals several hours after the following sunrise. The hours of sunset and sunrise were recorded for each trial and were corroborated from the ITAG's ambient light sensor readings. These time stamps were used to segment a full trial into day and night sections.

Statistical analyses

Following behavioral classification, ODBA amplitude during various behaviors (e.g. ascending and descending, forward and backward swimming) and the daily cycle (e.g. day and night) were then used to identify differences in activity level during behavioral modes. Statistical analysis of the ODBA values in relation to the movement, orientation and diel cycle was applied using a generalized linear mixed-effects (GLME) model in MATLAB, considering our ∼113 h dataset as a mixed dataset that has both random and fixed effects (fixed comparison between categories: ascent/descent, arms/mantle, day/night; random effect: variation among different squid). GLME models describe the relationship between a response variable and independent variables using coefficients that can vary with respect to one or more grouping variables for data with a response variable distribution that is not normal. In our model, ODBA peak amplitude was the response variable, the three categories (ascent/descent, arms/mantle, day/night) were, respectively (during each comparison), the predictor variables, and squid ID (1–7) was the grouping variable. The analysis fitted a GLME model for ODBA amplitude per category, with the same fixed-effects term and potentially correlated random effect for category grouped by individual squid.

Journal of Experimental Biology (2019) 222, jeb198226. doi:10.1242/jeb.198226

RESULTS

Classification accuracy and gait identification

The decision tree gait classifier was applied to analyze the accelerometry data from the seven tagged squid. Each 1 s window of the accelerometry data was classified as finning, flapping or jetting as described in Materials and Methods (Fig. 3). Finning behaviors exist along a continuum and were visibly similar, characterized by undulatory fin movement with at least one full wavelength present on the fin chord. Qualitatively, finning more often corresponded to semi-stationary, hovering behavior or slow translation. Flapping and jetting behaviors were much less common and corresponded to high-speed maneuvers.

The videos of the squid were analyzed and each gait event with the tagged squid in the video frame was given a gait label. The performance of the gait classifier compared with the human-labeled behaviors was visualized in a confusion matrix (Fig. 4B). The overall accuracy of the gait classifier was 99.6% (595 of 597 s classified correctly). The algorithm had high classification accuracy for finning and jetting gaits (100%: 573 of 573 correct; and 100%: 6 of 6 correct, respectively); flapping detection was slightly less accurate (89% or 16 of 18 correct). All misclassifications for the flapping gait were instead assigned to finning.

The classifier was used to analyze all gait events throughout the experiment, including those that were not captured on video. The three gait categories (finning, flapping, jetting) were identified in all seven tagged squid. ODBA values increased across the three gaits, from finning to jetting (Fig. 5A). Finning had a median ODBA value of 0.06 ***g*** [maximum 0.721 ***g***, interquartile range (IQR) 0.049 ***g***, minimum 0.000 ***g***], flapping had a median value of 0.123 ***g*** [maximum 0.961 ***g***, IQR 0.118 ***g***, minimum 0.003 ***g***], and jetting had a median value of 0.187 ***g*** [maximum 3.872 ***g***, IQR 0.147 ***g***, minimum 0.001 ***g***] (Fig. 5B). Finning events were detected most often (Fig. 6), followed by flapping and jetting. Proportionally, tagged animals spent the vast majority of time finning (98%), and a much smaller portion of time flapping (1%) or jetting (1%) (Fig. 6B).

Vertical and horizontal motion

The ITAG's pressure sensor provided information about vertical movements in the tank, and ODBA was used to estimate the swimming effort of the animal during ascent and descent (Fig. 7A,B). Statistical differences between ascent and descent were identified between ascending and descending ODBA values across the seven tagged squid. Ascending ODBA values for all squid (Fig. 7B) revealed a median peak value of 0.108 ***g*** [maximum 0.241 ***g***; IQR 0.064 ***g***; minimum 0.006 ***g***]. Descending motion showed a significantly lower (GLME test; *P*-value for fixed effect=1.14e−07) median peak value of 0.096 ***g*** [maximum 0.220 ***g***; IQR 0.061 ***g***; minimum 0.00 ***g***].

Direction of travel

Pitch data acquired by the ITAG's accelerometers provided information on the direction of movement with respect to the body of the animal (arms-first versus mantle-first swimming behavior). The pitch-threshold classifier described in Materials and Methods was applied to analyze the accelerometry data from the seven tagged squid. Each 1 s window of the accelerometry data was classified as either arms-first or mantle-first swimming (Fig. 3). Independently, the video of the squid was analyzed by a human observer and each 1 s event with the tagged squid in the frame was given a direction of travel label. The overall accuracy of the direction of travel classifier was 94.4% (771 of 817 s classified correctly).

Peak ODBA values during both arms-first and mantle-first swimming varied (Fig. 7C), and arm- and mantle-first swimming motions were statistically different (Fig. 7D; GLME test; *P*-value for fixed effect=0.019). Arms-first swimming had a lower median peak value of 0.099 ***g*** [maximum 0.220 ***g***; IQR 0.059 ***g***; minimum 0.005 ***g***], while mantle-first swimming had a higher median peak value of 0.102 ***g*** [maximum 0.241 ***g***; IQR 0.033 ***g***; minimum 0.003 ***g***].

An analysis of the duration of arms-first and mantle-first swimming events revealed that the tagged squid spent a consistent amount of time swimming in a single direction before switching directions throughout the 113 h of total experimental time. The mean duration of arms-first and mantle-first swimming events was similar, at 9.7±7.57 and 9.02±6.71 s, respectively. The frequency of orientation changes was likely caused by the size of the experimental tank; squid were observed to swim to the end of the tank before reversing direction and returning across the tank. The data confirm that the squid did not prefer one swimming orientation over the other. The total time spent in arms- and mantle-first orientations was approximately equal when summed across all seven squid: arms-first behavior was observed for a total time of 58 h 32 min 20 s and mantle-first swimming for a total time of 54 h 26 min 40 s (Fig. 8).

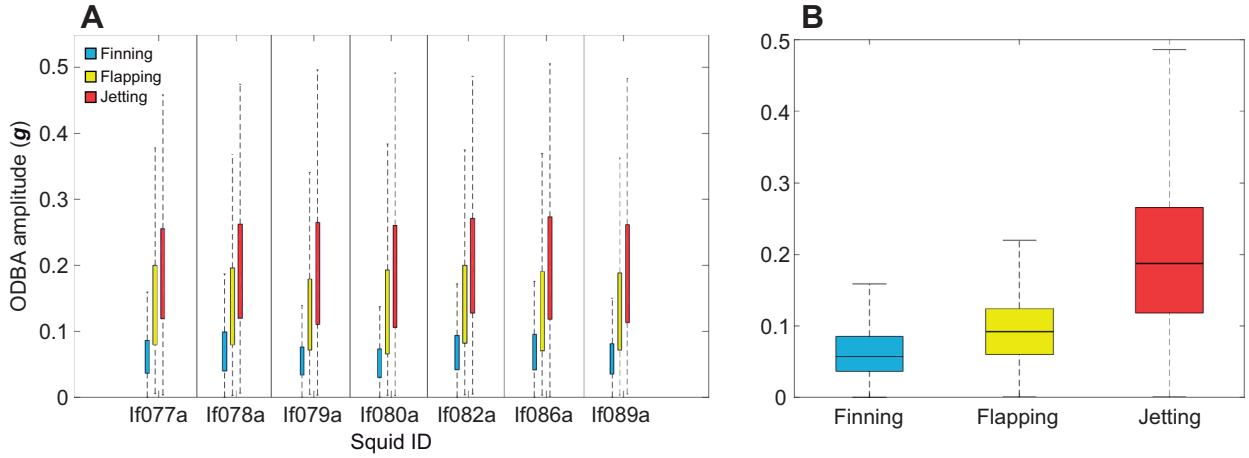

Fig. 5. Gait classification. (A) Boxplots of the different gaits for each individually tagged squid. (B) Boxplot showing the distribution of the ODBA peak values for all tagged squid using different gaits. For boxplots, the central mark indicates the median (not shown in A), and the bottom and top edges of the box indicate the 25th and 75th percentiles, respectively. Error bars indicate the range of values for peak ODBA amplitude for each swimming gait behavior; outliers were not plotted.

Journal of Experimental Biology (2019) 222, jeb198226. doi:10.1242/jeb.198226

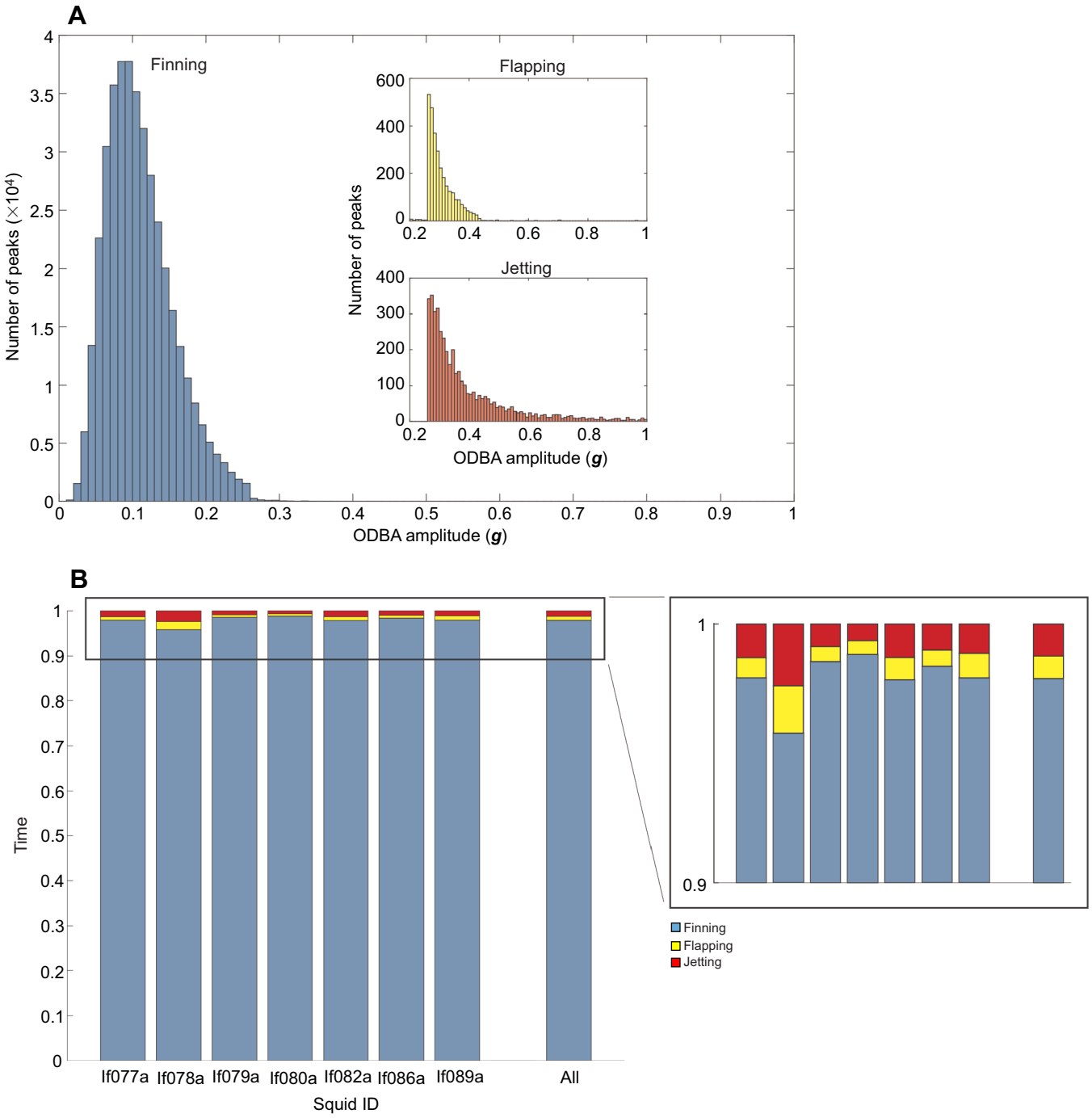

Fig. 6. Number of events and daily gait budgets. (A) Histogram illustrating the number of identified events for all animals examined in this study, categorized as finning, flapping and jetting. Each gait event was classified using the decision tree gait classifier based on both the ODBA magnitude and ODBA frequency response. While finning was observed across a wide range of peak ODBA values, flapping and jetting were observed only at higher ODBA values. (B) The time budget of the different gaits showing the proportion of time spent for each locomotive gait across the experiment.

Diel behavior

Animals also showed differences in diel patterns (Fig. 7E) across the five squid that carried a tag through a full day–night cycle. Significantly higher values of peak ODBA amplitude (GLME test; *P*-value for fixed effect=0.008) were found during the night (Fig. 7F), with median peak ODBA amplitude at 0.103 ***g*** [maximum 0.240 ***g***; IQR 0.066 ***g***; minimum 0.002 ***g***]. During the daytime, median peak ODBA acceleration amplitude was 0.098 ***g*** [maximum 0.222 ***g***; IQR 0.061 ***g***; minimum 0.005 ***g***].

DISCUSSION

New methods that enable the long-term persistent monitoring of animals in their natural environment are vital to answering fundamental questions about their behavior and mechanics, particularly for taxa that are difficult to observe like squid. Biologging tags are a key technology to tackle this problem, but the physical and environmental constraints on their design and functionality are a major problem. For squid, these constraints include minimizing the impact of the tag on behavior and swimming

Journal of Experimental Biology (2019) 222, jeb198226. doi:10.1242/jeb.198226

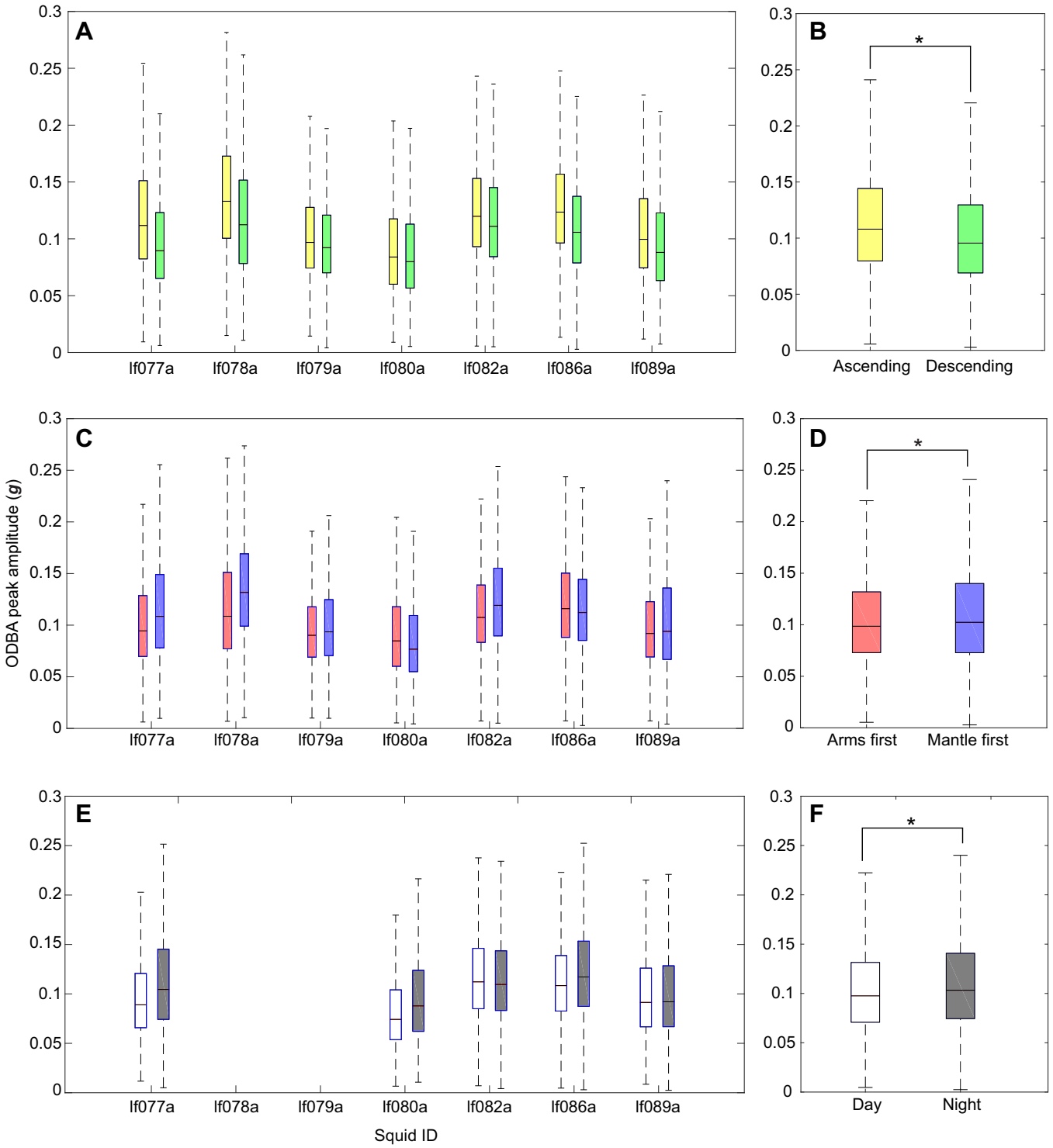

Fig. 7. Movement and orientation. Visualization of the ODBA peak values, grouped by various behaviors and across the seven individual squid. These data exhibit variation in value both between individual squid and across all squid in each behavior category. Significant differences (GLME test; $P<0.05$ for fixed effect) across all squid are denoted with asterisks. (A,B) Differences during ascent (yellow) and descent (green) in peak ODBA values for each tagged squid (A) and for all animals (B). (C,D) Peak ODBA amplitude during forward (arms first; red) and backward (mantle first; purple) motion for individual animals (C) and for all animals (D). (E,F) Differences in overall activity level during the day and night for both individual animals (E) and the group (F). In each subplot, the central mark indicates the median, and the bottom and top edges of the box indicate the 25th and 75th percentiles, respectively. Error bars indicate the range of values for peak ODBA amplitude for each swimming gait behavior; outliers were not plotted.

mechanics and functioning in the harsh marine environment. These constraints limit the type, number and location of the sensors used to measure behavior. Compact, low-power and robust microelectromechanical systems (MEMS) accelerometers lend themselves particularly well for persistent monitoring of small animals for days or weeks at a time, but without additional sensors

Journal of Experimental Biology (2019) 222, jeb198226. doi:10.1242/jeb.198226

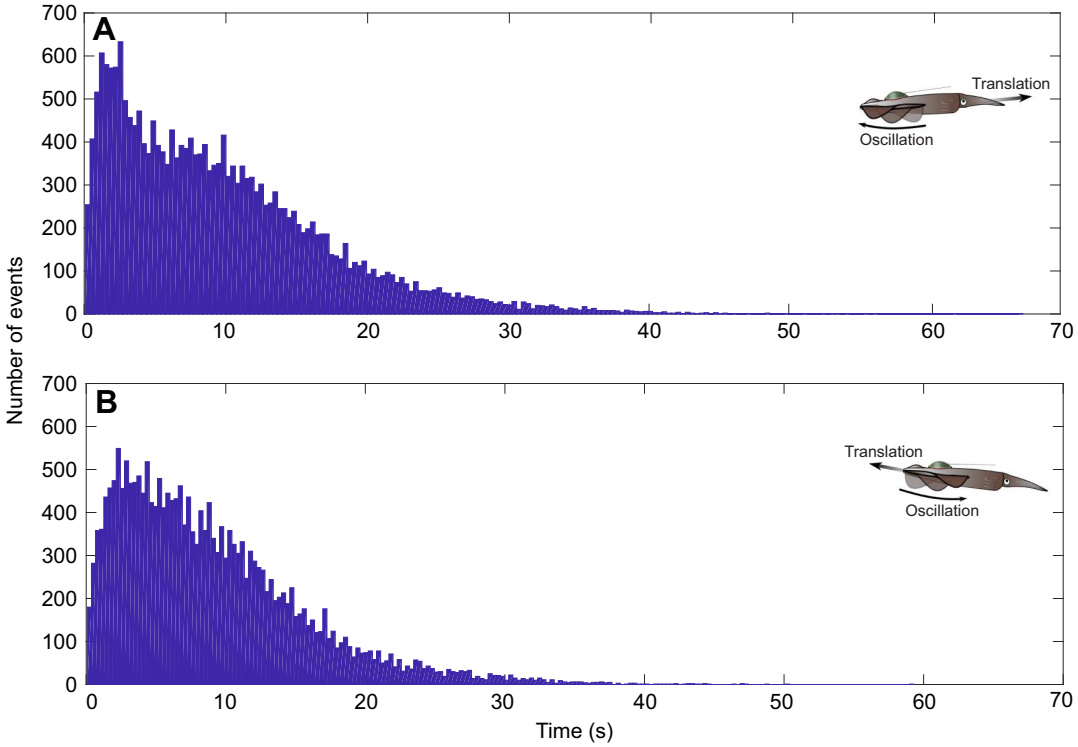

Fig. 8. Number of events and length of detection. Histograms showing the duration of the events detected as arms first (A) and mantle first (B) for all tagged squid (*n*=7). The mean (±s.d.) duration of arms-first events prior to switching to mantle-first swimming was 9.7±7.57 s, and squid spent 58 h 32 min 20 s in the arms-first orientation. The mean (±s.d.) duration of mantle-first swimming was 9.02±6.71 s, with a total time of 54 h 26 min 40 s spent in the mantle-first orientation.

it can be difficult to infer behavior from accelerometry alone. Pressure and magnetometer measurements are often used to complement measures of acceleration and, when fused together, result in the location of the animal in the water column, orientation (pitch, roll and yaw) and estimates of specific acceleration that result from locomotion. When combined with anthropometric data, the magnitude and the frequency of the specific acceleration can be used to estimate tail beat frequency, swimming speed and energetics in fish (Broell et al., 2013; Drucker, 1996; Wright et al., 2014). Importantly, these estimates and correlations with measurable parameters were both developed and verified in controlled experimental environments before they were used in environments where animals cannot be observed directly. Here, we successfully applied similar methodology to create and then verify the accuracy of algorithms that can identify and classify squid swimming gait from tag data. These algorithms are key to quantifying locomotion in free-swimming animals, and are an important first step in the development of a framework to quantify locomotion and energetics in free-swimming squid (Cooke et al., 2016).

The tag used in this work archives high-resolution (250 Hz) motion data for up to 36 h at a time. Deployments were kept to ca. 24 h for consistency and to observe tag detachment. The attachment method used (suturing to the dorsal surface of the mantle) provided a fixed position that likely reduced accelerometer noise. This enabled the acquisition of high-quality day-scale data that facilitated the development of a classifier for the identification and analysis of daily activity patterns in squid. Using the accelerometry-based tag sensor data, we were able to accurately classify three distinct swimming gaits with an overall 99% accuracy. Additionally, we were able to visualize and understand the continuum of dynamic acceleration observed during the finning gait and determine the swimming direction (arms first versus mantle first). In the constrained tank environment, finning was by far the most common gait for tagged squid. The jetting gait, which corresponded to high-energy maneuvers with no finning contribution, is presumed to be a costly mode of locomotion (O'Dor and Webber, 1986), seemed to increase ODBA and occurred rarely.

Notably, the jetting gait we have singled out here was a strong escape jet. Other studies have shown that some squids produce multiple jet patterns (Bartol et al., 2016, 2009; O'Dor, 1988) and high-acceleration jets are observed in the jetting gait and probably lower amplitude and perhaps graded jets are present in the fin-defined gaits. Finning behaviors had significantly lower estimates of specific acceleration (ODBA values), suggesting that movement preferences may also be related to energetic cost. The finning and flapping gaits were not likely substantially different from those observed in other squid species (Anderson and Demont, 2005; O'Dor, 1988; Stewart et al., 2010), although gait and locomotion are somewhat specific to species, their buoyance and fin morphology; and our observation methods differed as well. Our finning gaits appeared similar to mode II gait (both tail- and arms-first swimming) observed in *L. brevis* (Stewart et al., 2010). The flapping we observed occurred in both head- and tail-first directions and was similar to mode III and IV gaits. While these characterizations are useful to address behavioral patterns, it is vital to note that there was certainly a gradient between gaits, discernible in part by the ODBA continuum (Fig. 6) and the blending of finning and flapping noted elsewhere (e.g. mode III; Stewart et al., 2010). Thus, clear characteristics, such as ODBA amplitude, provide ways to compare across animals, lab to field, and perhaps across taxa.

Overall, the classifier was able to automatically identify different gaits with high accuracy. Classification accuracy was highest for the most frequently observed finning and the high-acceleration jetting, and lower for the intermediate flapping gait. All gaits were classified

with much higher accuracy than the 33% accuracy achievable by a random classifier, indicating that the classifier was able use the provided features to distinguish between gaits. Although paired video recordings and tag data were needed to develop the algorithm, the classifier was then used to classify gait events from tag data alone. Given that the experimental dataset consisted of over 113 h of experimental time, during much of which the squid were not clearly visible in the camera frame, the ability to autonomously determine gait from accelerometry data alone was vital.

Extending this work to automatically classify gaits in wild squid – when ground-truth gait information is unavailable – will require careful consideration of the trade-off faced by all machine learning models between accuracy on the given data and accurate generalization to unseen data. Generally, more complex models perform better on the observed data but may generalize poorly to new data; simpler models may have more consistent generalization performance, but can suffer from low accuracy on observed data. For the decision tree classifier applied in this work, model complexity corresponds to the number of 'splits' or levels in the decision tree. Although the decision tree was also able to generalize well on experimental data, choosing the best model to maintain high generalization performance on wild squid may require using a more or less complex decision tree model. Model complexity should be considered carefully before extending gait models to classify gait events in wild squid.

During all swimming gaits, animals were observed to ascend and descend in the water column and tended to spend nearly equivalent time in the arms- versus mantle-first orientations. Estimates of dynamic acceleration were higher as the animals moved up in the water and lower when descending. Video and tag data showed that the animals actively fin during both ascent and descent, but the lower ODBA values during descent suggest that descent is powered at least partially by the negative buoyancy of their bodies. This observation is consistent with climb and glide behaviors observed in tagged squid *in situ* (Gilly et al., 2006, 2012). The squid showed only a slight preference for the arms-first swimming orientation, spending 52% of the experimental time in the arms-first orientation. Arms-first swimming would position the head and eyes to provide a greater field of view, an important consideration for an animal that relies on its vision for survival and foraging (Shashar et al., 1998). Our data suggest that these squid did not significantly prefer arms-first swimming, suggesting that there may be other reasons for preferring a mantle-first orientation, or that the heightened visibility allowed by arms-first swimming is only desirable for specific behaviors, such as foraging, which was rarely observed in the tank-based experiments. Additionally, the confines of the tank-based experiment may have suppressed a clear preference for either swimming direction as the squid changed direction each time a tank boundary was encountered.

The animals were more active at night (Fig. 7). Like many other loliginids, *L. forbesii* are generally thought to migrate vertically and feed during the evening hours (O'Dor et al., 1995; Porteiro and Martins, 1994). During the daytime, we did not observe the resting behavior on the tank bottom that has been reported in other loliginids (Hanlon and Messenger, 1996). This lack of resting behavior was also reported in O'Dor et al. (1995), who found that *L. forbesii* hovered off the bottom of the tank – a metabolically costly behavior – and suggested this may be to avoid damage to skin or predation. Although it is difficult to know whether the high levels of daytime activity observed in our tank-based experiments are reflective of wild behavior, this behavior would agree with the putative daytime action of this species in the wild as inferred by the small commercial *L. forbesii* fishery in the Azores, in which squid are jigged for and caught during the day. This suggests squid themselves are actively hunting during the day. However, we did not visually observe any squid feeding during the day (which may reflect the animals' unrest with the surrounding activity instead of a real disposition against daytime feeding) but some did feed at night, as noted by the typical 'squid-bitten' fish remains in the morning. These combined observations would suggest that veined squid are active throughout the full diel cycle but increase their activity during the night. This pattern remains to be confirmed in the wild.

Fine-scale activity patterns revealed the prevalence of finning movements in tank-bound squid. In some respects this finning rate is surprising, because it has long been noted that fast, muscular, pelagic squid, such as *Illex illecebrosus* and *Doryteuthis opalescens*, rely on jetting, even at lower swim speeds (O'Dor and Webber, 1991; Webber and O'Dor, 1986). This jetting rate, at times, created a conundrum because jetting is not considered an efficient mode of transport (O'Dor et al., 1995; O'Dor and Webber, 1986; Vogel, 1994). Studies with smaller squid taxa, such as *L. brevis* and *D. pealeii*, revealed that finning is commonly used and is a relatively energetically efficient gait (Bartol et al., 2008, 2001). In actuality, jetting frequently occurs because it is coincident with respiration and mantle contractions, which is probably one reason it was often noted in previous studies (O'Dor and Webber, 1991; Webber and O'Dor, 1986). Rather, it might have been the methodological focus of the pressure sensor of the prior studies that only measured jetting and may have resulted in finning modes being overlooked. Our motion sensors and the high-speed camera data of others (Bartol et al., 2008, 2001) have helped reveal this additional insight into the occurrence rates of finning behaviors. Indeed, we predominantly observed undulatory and oscillatory finning in these large, tank-bound squid. Given that *L. forbesii* are negatively buoyant and are thus required to generate lift and offset drag (Anderson and Demont, 2005; Bartol et al., 2001), the finning rates noted here may offer performance that most efficiently combats those constraints. Whether finning occurs at a similar rate in the wild has yet to be seen, but the sheer dominance of this behavior in healthy, recently wild-caught squid certainly suggests that finning will also occur frequently in the field.

The ITAG and the development of other high sampling rate biologging tools and analysis algorithms are key to creating a system capable of providing insight into free-swimming squid behavior previously only accessible using high-resolution cameras, small tanks, DPIV methods (e.g. Anderson and Demont, 2005; Bartol et al., 2008) or lower sampling rate field observations (e.g. Gilly et al., 2012; Stewart et al., 2013). Here, we provide new analysis algorithms and a novel tag applied to a group of animals whose *in situ* behavior is difficult to observe. Although our experiments were conducted on captive squid, this work provides detailed observations of fine-scale behavioral patterns for *L. forbesii*. The general behavioral trends observed during this experiment, such as lower ODBA for descending behaviors and increased activity at night, align well with behaviors that have been observed in the field (e.g. Gilly et al., 2012).

Building on the gait classification data presented here, future work will be directed towards the experimental development of empirical relationships between parameters derived from tag results and the energetic cost associated with locomotion. The high temporal resolution sensors and tag utilized, coupled with the algorithms developed, can be used to understand organismal behavior in their natural environment. These laboratory results indicate a strong tendency to swimming modes with lower ODBA, and finning-based

movement occurred more often than previously proposed, at least for these large, negatively buoyant squid. The occurrence rates of other behaviors (arms-first swimming and lower ODBA), and higher ODBA at night and when ascending, provide new insight into squid ecophysiology that must be examined in the field.

Acknowledgements
The authors thank the scientific and technical staff at IMAR/DOP and Flying Sharks for their support with the experiments in the Azores, including A. Filipa, G. Graca, R. Prieto, J. Rodeia, N. Serpa, I. Martins, T. Morato, R. Guedes, A. Godinho, L. Silva, G. Graca, P. Martins and V. Rosa. The authors greatly appreciate the generous efforts and support of Flying Sharks and the Faial Nature Park for the use of the Porto Pim Aquarium and their assistance and patience during the trials.

Competing interests
The authors declare no competing or financial interests.

Author contributions
Conceptualization: G.E.F., T.A.M., K.K., J.F., P.A., K.A.S.; Methodology: G.E.F., F.C., T.A.M., K.K., J.F., P.A., K.A.S.; Software: G.E.F., F.C., K.A.S.; Validation: G.E.F., K.A.S.; Investigation: G.E.F., T.A.M., K.A.S.; Resources: T.A.M., J.F., P.A., K.A.S.; Data curation: G.E.F., F.C., K.A.S.; Writing - original draft: G.E.F., F.C., T.A.M., K.K., K.A.S.; Writing - review & editing: G.E.F., T.A.M., K.K., K.A.S.; Visualization: G.E.F., K.A.S.; Supervision: T.A.M., K.K., K.A.S.; Project administration: T.A.M., K.K., K.A.S.; Funding acquisition: T.A.M., K.K., K.A.S.

Funding
This work was supported by Woods Hole Oceanographic Institution's Ocean Life Institute and the Innovative Technology Program, Hopkins Marine Station's Marine Life Observatory (to K.K.), as well as the National Science Foundation Program for Instrument Development for Biological Research (award no. 1455593 to T.A.M., K.K. and K.A.S.). F.C. thanks the Presidentís International Fellowship Initiative (PIFI) of the Chinese Academy of Science. G.E.F. thanks the National Science Foundation GRFP and National Science Foundation REU programs for support of this research.

References
Anderson, E. J. and DeMont, M. E. (2000). The mechanics of locomotion in the squid Loligo pealei: locomotory function and unsteady hydrodynamics of the jet and intramantle pressure. *J. Exp. Biol.* **203**, 2851-2863.
Anderson, E. J. and DeMont, M. E. (2005). The locomotory function of the fins in the squid Loligo pealei. *Mar. Freshw. Behav. Physiol.* **38**, 169-189. doi:10.1080/10236240500230765
Anderson, E. J. and Grosenbaugh, M. A. (2005). Jet flow in steadily swimming adult squid. *J. Exp. Biol.* **208**, 1125-1146. doi:10.1242/jeb.01507
Bartol, S. M., Musick, J. A. and Lenhardt, M. L. (1999). Auditory evoked potentials of the loggerhead sea turtle (*Caretta caretta*). *Copeia* **3**, 836-840. doi:10.2307/1447625
Bartol, I. K., Patterson, M. R. and Mann, R. (2001). Swimming mechanics and behavior of the shallow-water brief squid Lolliguncula brevis. *J. Exp. Biol.* **204**, 3655-3682.
Bartol, I. K., Krueger, P. S., Thompson, J. T. and Stewart, W. J. (2008). Swimming dynamics and propulsive efficiency of squids throughout ontogeny. *Integr. Comp. Biol.* **48**, 720-733. doi:10.1093/icb/icn043
Bartol, I. K., Krueger, P. S., Stewart, W. J. and Thompson, J. T. (2009). Hydrodynamics of pulsed jetting in juvenile and adult brief squid Lolliguncula brevis: evidence of multiple jetmodes' and their implications for propulsive efficiency. *J. Exp. Biol.* **212**, 1889-1903. doi:10.1242/jeb.027771
Bartol, I. K., Krueger, P. S., Jastrebsky, R. A., Williams, S. and Thompson, J. T. (2016). Volumetric flow imaging reveals the importance of vortex ring formation in squid swimming tail-first and arms-first. *J. Exp. Biol.* **219**, 392-403. doi:10.1242/jeb.129254
Block, B. A. (2005). Physiological ecology in the 21st century: advancements in biologging science. *Integr. Comp. Biol.* **45**, 305-320. doi:10.1093/icb/45.2.305
Bograd, S. J., Block, B. A., Costa, D. P. and Godley, B. J. (2010). Biologging technologies: new tools for conservation. Introduction. *Endanger. Species Res.* **10**, 1-7. doi:10.3354/esr00269
Broell, F., Noda, T., Wright, S., Domenici, P., Steffensen, J. F., Auclair, J.-P. and Taggart, C. T. (2013). Accelerometer tags: detecting and identifying activities in fish and the effect of sampling frequency. *J. Exp. Biol.* **216**, 1255-1264. doi:10.1242/jeb.077396
Clarke, M. R. (1977). Beaks, nets and numbers. *Symp. Zool. Soc. Lond.* **38**, 89-126.
Cooke, S. J., Brownscombe, J. W., Raby, G. D., Broell, F., Hinch, S. G., Clark, T. D. and Semmens, J. M. (2016). Remote bioenergetics measurements in wild fish: opportunities and challenges. *Comp. Biochem. Physiol. A Mol. Integr. Physiol.* **202**, 23-37. doi:10.1016/j.cbpa.2016.03.022
Costa, D. P., Block, B., Bograd, S., Fedak, M. A. and Gunn, J. S. (2010). TOPP as a marine life observatory: using electronic tags to monitor the movements, behavior and habitats of marine vertebrates. *Proceed. OceanObs* **9**, 21-25. doi:10.5270/OceanObs09.cwp.19
Drucker, E. G. (1996). The use of gait transition speed in comparative studies of fish locomotion. *Am. Zool.* **36**, 555-566. doi:10.1093/icb/36.6.555
Gilly, W. F., Zeidberg, L. D., Booth, J. A. T., Stewart, J. S., Marshall, G., Abernathy, K. and Bell, L. E. (2012). Locomotion and behavior of Humboldt squid, *Dosidicus gigas*, in relation to natural hypoxia in the Gulf of California, Mexico. *J. Exp. Biol.* **215**, 3175-3190. doi:10.1242/jeb.072538
Gilly, W. F., Markaida, U., Baxter, C. H., Block, B. A., Boustany, A., Zeidberg, L. D., Reisenbichler, K., Robinson, B., Bassino, G. and Salinas, C. (2006). Vertical and horizontal migratoins by the jumbo squid *Dosidicus gigas* revealed by electronic tagging. *Mar. Ecol. Prog. Ser.* **324**. doi:10.3354/meps324001
Gleiss, A. C., Wilson, R. P and Shepard, E. L. (2011). Making overall dynamic body acceleration work: on the theory of acceleration as a proxy for energy expenditure. *Methods Ecol. Evolu.* **2**, 23-33.
Hanlon, R. and Messenger, J. B. (1996). *Cephalopod Behavior*. New York: Cambridge University Press.
Hussey, N. E., Kessel, S. T., Aarestrup, K., Cooke, S. J., Cowley, P. D., Fisk, A. T., Harcourt, R. G., Holland, K. N., Iverson, S. J. and Kocik, J. F. (2015). Aquatic animal telemetry: a panoramic window into the underwater world. *Science* **348**, 1255642. doi:10.1126/science.1255642
Jastrebsky, R. A., Bartol, I. K. and Krueger, P. S. (2016). Turning performance in squid and cuttlefish: unique dual mode, muscular hydrostatic systems. *J. Exp. Biol.* **219**, 1317-1326. doi:10.1242/jeb.126839
Jastrebsky, R., Bartol, I. and Krueger, P. (2017). Turning performance of brief squid Lolliguncula brevis during attacks on shrimp and fish. *J. Exp. Biol.* **220**, 908-919. doi:10.1242/jeb.144261
Johnson, M. P. and Tyack, P. L. (2003). A digital acoustic recording tag for measuring the response of wild marine mammals to sound. *IEEE J. Ocean. Eng.* **28**, 3-12. doi:10.1109/JOE.2002.808212
Kaplan, M. B., Mooney, T. A., McCorkle, D. M. and Cohen, A. (2013). Adverse effects of ocean acidification on early development of squid (*Doryteuthis pealeii*). *PLoS ONE* **8**, e63714. doi:10.1371/journal.pone.0063714
Kotsiantis, S. B. (2013). Decision trees: a recent overview. *Artif. Intell. Rev.* **39**, 261-283. doi:10.1007/s10462-011-9272-4
Mooney, T. A., Katija, K., Shorter, K. A., Hurst, T., Fontes, J. and Afonso, P. (2015). ITAG: an eco-sensor for fine-scale behavioral measurements of soft-bodied marine invertebrates. *Animal Biotelemetry* **3**, 1-14. doi:10.1186/s40317-015-0076-1
Nathan, R., Spiegel, O., Fortmann-Roe, S., Harel, R., Wikelski, M. and Getz, W. M. (2012). Using tri-axial acceleration data to identify behavioral modes of free-ranging animals: general concepts and tools illustrated for griffon vultures. *J. Exp. Biol.* **215**, 986-996. doi:10.1242/jeb.058602
O'Dor, R. (1988). The forces acting on swimming squid. *J. Exp. Biol.* **137**, 421-442.
O'Dor, R. and Webber, D. (1991). Invertebrate athletes: trade-offs between transport efficiency and power density in cephalopod evolution. *J. Exp. Biol.* **160**, 93-112.
O'Dor, R. K. and Webber, D. M. (1986). The constraints on cephalopods: why squid aren't fish. *Can. J. Zool.* **64**, 1591-1605. doi:10.1139/z86-241
O'Dor, R. K., Hoar, J. A., Webber, D. M., Carey, F. G., Tanaka, S., Martins, H. R. and Porteiro, F. M. (1995). Squid (*Loligo forbesi*) performance and metabolic rates in nature. *Mar. Freshw. Behav. Physiol.* **25**, 163-177. doi:10.1080/10236249409378915
O'Dor, R., Adamo, S., Aitken, J., Andrade, Y., Finn, J., Hanlon, R. and Jackson, G. (2002). Currents as environmental constraints on the behavior, energetics and distribution of squid and cuttlefish. *Bull. Mar. Sci.* **71**, 601-617.
Porteiro, F. M. and Martins, H. (1994). Biology of *Loligo forbesi* Steenstrup, 1856 (Mollusca:Cephalopoda) in the Azores: sample composition and maturation of squid caught by jigging. *Fish. Res.* **21**, 103-114. doi:10.1016/0165-7836(94)90098-1
Pörtner, H. (2002). Environmental and functional limits to muscular exercise and body size in marine invertebrate athletes. *Comp. Biochem. Physiol. A Mol. Integr. Physiol.* **133**, 303-321. doi:10.1016/S1095-6433(02)00162-9
Pörtner, H., Langenbuch, M. and Reipschläger, A. (2004). Biological impact of elevated ocean CO2 concentrations: lessons from animal physiology and earth history. *J. Oceanogr.* **60**, 705-718. doi:10.1007/s10872-004-5763-0
Rosa, R. and Seibel, B. A. (2010). Metabolic physiology of the Humboldt squid, *Dosidicus gigas*: Implications for vertical migration in a pronounced oxygen minimum zone. *Prog. Oceanogr.* **86**, 72-80. doi:10.1016/j.pocean.2010.04.004
Rosa, R., Trübenbach, K., Pimentel, M. S., Boavida-Portugal, J., Faleiro, F., Baptista, M., Dionísio, G., Calado, R., Pörtner, H. O. and Repolho, T. (2014). Differential impacts of ocean acidification and warming on winter and summer progeny of a coastal squid (*Loligo vulgaris*). *J. Exp. Biol.* **217**, 518-525. doi:10.1242/jeb.096081
Shashar, N., Hanlon, R. T. and Petz, A. M. (1998). Polarization vision helps detect transparent prey. *Nature* **393**, 222. doi:10.1038/30380
Shepard, E. L., Wilson, R. P., Halsey, L. G., Quintana, F., Laich, A. G., Gleiss, A. C., Liebsch, N., Myers, A. E. and Norman, B. (2008). Derivation of body motion via appropriate smoothing of acceleration data. *Aquatic Biol.* **4**, 235-241.

Shorter, K. A., Shao, Y., Ojeda, L., Barton, K., Rocho-Levine, J., van der Hoop, J. and Moore, M. (2017). A day in the life of a dolphin: using bio logging tags for improved animal health and well being. *Mar. Mamm. Sci.* **33**, 785-802. doi:10.1111/mms.12408

Stark, K. E., Jackson, G. D. and Lyle, J. M. (2005). Tracking arrow squid movements with an automated acoustic telemetry system. *Mar. Ecol. Prog. Ser.* **299**, 167-177. doi:10.3354/meps299167

Stewart, W. J., Bartol, I. K. and Krueger, P. S. (2010). Hydrodynamic fin function of brief squid, Lolliguncula brevis. *J. Exp. Biol.* **213**, 2009-2024. doi:10.1242/jeb.039057

Stewart, J. S., Field, J. C., Markaida, U. and Gilly, W. F. (2013). Behavioral ecology of jumbo squid (*Dosidicus gigas*) in relation to oxygen minimum zones. *Deep Sea Res. II* **95**, 197-208. doi:10.1016/j.dsr2.2012.06.005

Vogel, S. (1994). *Life in Moving Fluids: The Physical Biology of Flow*. Boston, MA: Willard Grant Press.

Webber, D. M. and O'Dor, R. K. (1986). Monitoring the metabolic rate and activity of free-swimming squid with telemetered jet pressure. *J. Exp. Biol.* **126**, 205-224.

Wilson, R. P., White, C. R., Quintana, F., Halsey, L. G., Liebsch, N., Martin, G. R. and Butler, P. J. (2006). Moving towards acceleration for estimates of activity-specific metabolic rate in free-living animals: the case of the cormorant. *J. Anim. Ecol.* **75**, 1081-1090. doi:10.1111/j.1365-2656.2006.01127.x

Wright, S., Metcalfe, J. D., Hetherington, S. and Wilson, R. (2014). Estimating activity-specific energy expenditure in a teleost fish, using accelerometer loggers. *Mar. Ecol. Prog. Ser.* **496**, 19-32. doi:10.3354/meps10528